이학석사 학위논문

Enhanced Absorption of Liquid Thin Layer on Terahertz Nanoantennas

테라헤르츠 나노 안테나 위 액체막의 흡수 증가

2014년 2월

서울대학교 대학원

물리천문학부

정 지 윤

Enhanced Absorption of Liquid Thin Layer on Terahertz Nanoantennas

지도 교수 김 대 식

이 논문을 이학석사 학위논문으로 제출함
2014년 2월

서울대학교 대학원
물리천문학부
정 지 윤

정지윤의 이학석사 학위논문을 인준함
2014년 2월

위 원 장 _____ (인)

부위원장 _____ (인)

위 원 _____ (인)

Abstract

Absorption of terahertz electromagnetic waves by liquid thin layers on metallic nano-slot antennas is investigated. Nano-slot antennas, metallic film with holes of nanometer-sized slots, are known to show strong resonance at certain frequency, and sensitivity to the dielectric environment. Liquid thin layer is formed using spin-coated PDMS and patterned silicon oxide, which prevent liquids from smearing out. In the presence of liquids the transmission spectra of nano-slot antennas show large amplitude modulations and peak shifts according to the dielectric properties of the liquids. The tendency becomes larger with smaller antenna width. With further optimizations in sealing and antenna structure, this scheme is expected to open up the possibility of measuring much more minute samples, such as a few-layer molecule layer.

Keywords : Terahertz Spectroscopy, Liquids, Nano-slot antenna
Student Number : 2012-20387

Contents

1. Introduction..... 3

2. Terahertz Nanoantenna 7

2.1. Resonance Behavior of Terahertz Slot Antenna.....8

2.2. Field Enhancement in Terahertz Nanoantenna 11

2.3. Terahertz Nanoantenna for sensing application 14

3. Terahertz Spectroscopy on Liquids.....15

4. Experiment 17

4.1. Experimental Setup.....18

4.2. Terahertz Nanoantenna 20

4.3. Cover Layer 23

5. Results.....25

5.1. Terahertz Properties of Bulk Liquid 26

5.2. Terahertz Nanoantenna Measurement.....28

5.3. Water Thin layer on Terahertz Nanoantennas 30

6. Summary 34

7. References.....36

1. Introduction

Discovery of surface plasmon (1), a surface-bound state of collective electron oscillation, opened a new field in studies on interactions of metals with electromagnetic fields. Among many interesting phenomena induced by surface plasmons one of the most extensively investigated fields is extraordinary transmission of light (2). Since surface plasmons can only appear in lossy metals, studies on optical properties of subwavelength metallic structures have been mainly focused in visible and infrared frequency range (3, 4). Recently it has been theoretically and experimentally investigated that extraordinary transmission can also appear in low frequency region including far-IR and terahertz, where noble metals can be approximated as perfect electric conductors (PEC) (5, 6). This greatly extends the frequency range where subwavelength metallic structures can be used. The squeezing of light through subwavelength gaps therefore provides an attractive solution to spectroscopic applications, such as SERS (7, 8) and SEIRA (9), requiring amplification of detection signals.

Terahertz spectroscopy, which is capable of detecting intermolecular vibrational modes with time scales on the order of picosecond (10), therefore can also benefit from the extraordinary transmission. Absorption coefficients of

intermolecular vibrational modes are usually in the order of a few tens of wavenumbers (11), which means that tens of milligrams of molecules are needed for detection. Plasmonic nanoantennas, metallic nanostructures with strong local field near their structures, enhance absorption signals by a few orders of magnitude and help one overcome the limited detectability of molecules (12, 13). Especially when negative slot antenna is adopted for the nanostructure, more quantitative analysis is possible due to the well-defined volume inside the slot.

The absorption enhancement induced by the plasmonic nanoantennas can also be of use in fluidic applications. Since the response of nanoantennas to the incident field changes dramatically with the dielectric environment near their structures (14), nanoantennas can help detect and analyze the state of target liquid sensitively, even when the amount of liquid is small. The nanoantenna-liquid system is widely acknowledged for its potential to be applied in detecting analytes (15) and even in tracing chemical reactions in real time (16). Most of the reported experimental schemes for nanoantenna-liquid system, however, adopt reflection or scattering geometry. Since there are many cases where

transmission geometry is useful for further quantitative analysis (17), it is also necessary to develop a scheme compatible with transmission experiments.

In this thesis terahertz transmission spectrum of liquid thin layer on metallic nanoantennas is measured. Liquid thin layer is formed by sandwiching the liquid between cover layer and the nanoantennas. Since terahertz nanoantennas are very sensitive to dielectric environment, thin liquid layers are expected to be more distinguishable in the presence of the nanoantennas. Further optimizations on antenna width and liquid confinement can pave the way to measuring a single molecule or a few layers of liquid in transmission scheme.

2. Terahertz Nanoantenna

2.1. Resonance Behavior of Terahertz Slot Antenna

Optical properties of metals such as electric permittivity and skin depth show huge dependence on the frequency of incident light (18). For instance noble metals become transparent at UV, although opaque at visible frequencies. In low-frequency regime of IR or terahertz, noble metals show negligible absorption loss and therefore can be approximated as perfect electric conductor (PEC). Due to such a behavior slot antennas are very efficient in concentrating electromagnetic field in terahertz frequency, since there would be only negligible loss from the antenna itself.

Being the Babinet complement of optical dipole antenna (19), slot antenna is capable of coupling electromagnetic waves efficiently into its structure. In case of an asymmetric rectangular slot, transmission at resonance is analytically approximated as below (20).

$$T_{res} \simeq \frac{3}{4\pi}\frac{\lambda_{res}^2}{a_x a_y} \simeq \frac{3}{\pi}\frac{a_y}{a_x}$$

Here a_x and a_y refer to length of short and long side of the rectangle, respectively, and resonance wavelength $\lambda_{\mathrm{res}} \simeq 2a_y$.

This implies that the asymmetry of the rectangular slot determines the enhancement of the electromagnetic field inside, which was experimentally confirmed up to ratio of $\mathrm{a_y} = 30a_x$ using terahertz near-field imaging (21).

In the presence of a substrate, as in most cases, resonance behavior of a terahertz slot antenna depends on both refractive index of the substrate and structure of the antenna. In case of a thin metal film the normalized energy flow is approximated as below (14).

$$S_z^{norm} = \frac{32}{\pi^2} \frac{Re(W_3)}{|W_1 + W_3|^2}$$

Here W is coupling strength between incident electromagnetic field and internal mode of the slot at the air-aperture (W_1) or aperture-substrate (W_3) interface, which depends on slot shape parameters and the dielectric constants of the substrate. The overall effect of substrate comes out as shifting the resonance wavelength to $\lambda_{res} = 2n_{eff}a_y$, where n_{eff} varies from 1 to $n_{substrate}$.

H. R. Park et al. (22) reported that thickness of the substrate also influences the resonance behavior of the slot antenna. The resonance wavelength is blueshifted as the width of the slot increases or the thickness of the substrate decreases. Noting

that coupling between internal modes of the slot and dielectric environment at the output (W_1, W_3) determines the resonance, one can think of thinner slot to be less influenced by the finite thickness of the substrate; in other words detect thin substrate better.

2.2. Field Enhancement in Terahertz Nanoantenna

As mentioned before, field enhancement inside a slot antenna is determined by the asymmetry of the slot structure. For a fixed resonance frequency, therefore, reducing the gap size leads to higher field enhancement. Local terahertz electric field enhancement of 800 was reported in 70nm gap (23) and 25,000 in one-nanometer gap structure (24). It is notable that electromagnetic wave manages to pass through a gap 3,000,000 times smaller than its wavelength, which is counterintuitive considering the calculations by Bethe.

It can be intuitively understood that such an enhancement comes from capacitive effect, where incident light drives the surface current and charges accumulate at the edge of the antenna, which in turn produce strong electric field inside the gap (23). In case of infinite slit, therefore, the transmission spectrum will show inversely proportional behavior with respect to frequency of the incident light. Local capacitor model successfully predicts the field enhancement invoking the concept of λ-zone (25).

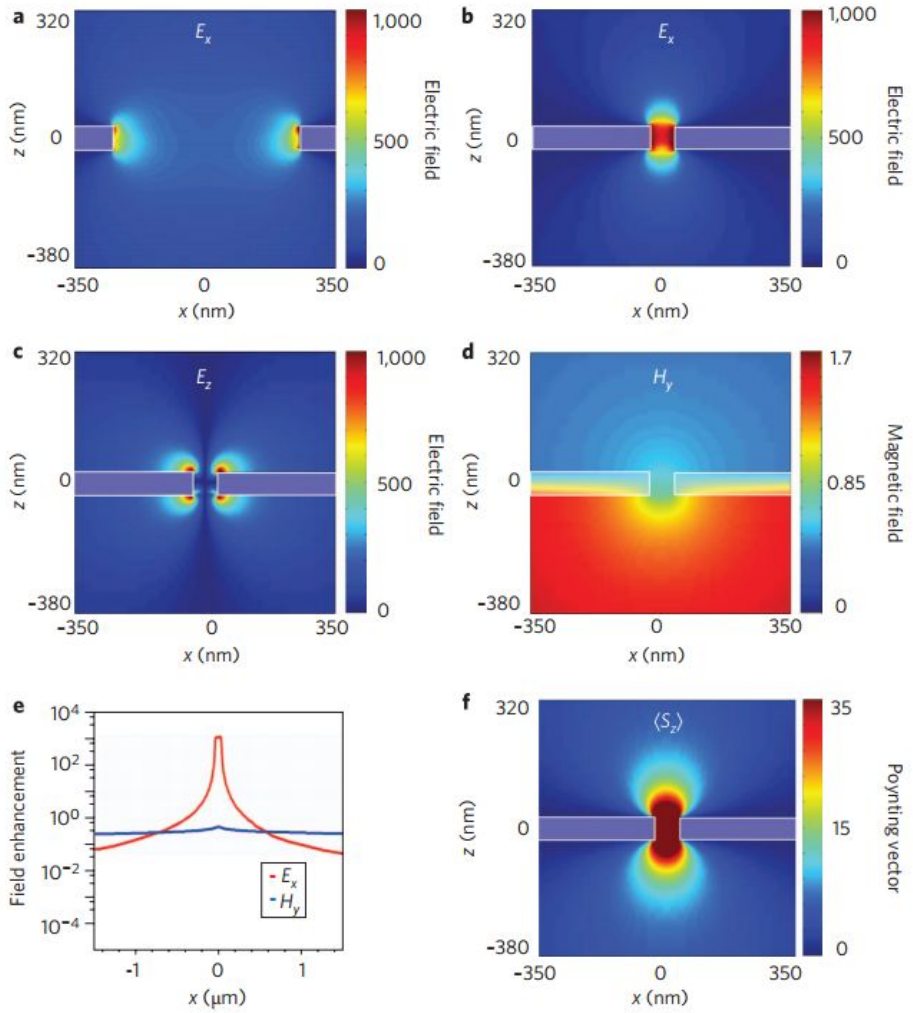

Figure 1 Simulated field around 500nm / 70nm gap structure.

(Image from ref. 23)

The enhanced field is strongly localized inside the slot. Figure 1 depicts the field profile near the gap structure. The enhanced field rapidly diminishes outside the gap, which infers that only those inside the gap will benefit from the strong field generated by antennas.

There is another interesting aspect about the field enhancement

inside a gap structure. Transverse electric field is enhanced by a factor up to 1000, while magnetic field remains within a factor of 2 caused by reflection from the metal surface. Such asymmetric behaviors of electric and magnetic field, along with the localized properties of the enhanced field, make the slot antennas ideal tool for quantitative sensing applications.

2.3. Terahertz Nanoantenna for sensing application

Larger field enhancement results in more coupling between the electromagnetic field and the material inside the antenna. This therefore can be applied for amplifying signal that was too small to be detected before. For example Raman scattering signal is proportional to $|E|^4$ while energy from incident light scales as $|E|^2$; this is what makes surface-enhanced Raman spectroscopy (SERS) possible (26).

H. R. Park et al. (17) reported that same logic can also be applied in absorption processes where a molecule with electric dipole μ interacts with an electromagnetic wave with electric field E. From the Fermi golden rule the absorption cross section can be written as follows.

$$\sigma = \frac{2\pi}{\hbar}\,\mu^2 E^2 \rho(\hbar\omega_0)\frac{\hbar\omega_0}{S} \propto \frac{E^2}{S}$$

Due to the asymmetric electromagnetic environment explained in the previous chapter, the ratio E^2/S is shifted from the free space value of Z_0 ($Z_0 = 377\Omega$), thereby increasing the absorption cross section by orders of three in case of 50nm width slot. 22fg of RDX molecules could be detected in this way, despite its relatively small absorption coefficient value of $50cm^{-1}$.

3. Terahertz Spectroscopy on Liquids

In condensed matter physics interactions of terahertz photons with transverse-optical phonons (27), free carriers in doped semiconductor (28), and excitons (29) have been extensively studied and physically understood. Terahertz spectroscopy on liquids, on the other hand, usually suffers from lack of analytical models that can describe the dielectric spectrum (30). For example, liquid water has an absorption band at $180cm^{-1}$ that can be explained by either of the following: H-bond stretching, restricted translation parallel to OH - O, O-O stretch, or longitudinal phonon etc. (31). Along with peak broadening this makes analysis of terahertz spectrum of liquid somewhat ambiguous.

Despite such and other shortcomings terahertz spectroscopy on liquids is of great importance in chemistry and biology. Terahertz spectroscopy detects interactions between molecules and therefore it can be used to analyze the dynamics of molecules in solvent. For example a hydrogen bond, which is responsible for many interesting molecular dynamics such as hydration water (32), can be detected in terahertz frequency. In order to gain further insight into the dynamics of molecules in liquid state, it is therefore mandatory to understand the properties of liquid itself in the terahertz regime first.

4. Experiment

4.1. Experimental Setup

To obtain terahertz transmission characteristics of samples, terahertz time-domain spectroscopy (THz-TDS) is used. TDS measures the electric field as a function of time, and take its Fourier transform to obtain the spectrum. Since a pulse in time-domain contains information on both the phase and the amplitude, it is possible to measure both the refractive index and the absorption coefficient of the sample.

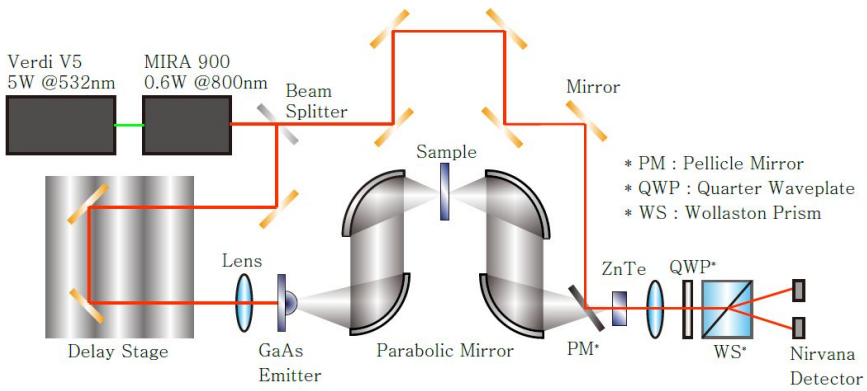

Figure 2 Experimental setup for terahertz time-domain spectroscopy.

The experimental setup is shown in figure 1. Ti:Sapphire oscillator MIRA 900 is pumped by 5W 532nm laser Verdi V5 to generate 80MHz repetition rate, 130fs duration pulsed beam of 0.6W with center wavelength of 800nm. Passing a beam splitter the pulsed beam is split into pump beam (headed to the bottom)

and probe beam (to the right). Terahertz pulse is generated as the pump beam hits the 150V-biased GaAs emitter, and then collected by parabolic mirrors.

THz pulse signal is measured with electro-optic (EO) method, which utilizes the EO material whose optical refractive index changes proportional to the amplitude of incident THz electric field (33). The probe beam, whose polarization changes due to the incident THz pulse, becomes circularly polarized by passing quarter wave plate. Wollaston prism divides the beam into two orthogonally polarized components, the difference of whose energies is proportional to the amplitude of incident THz field and is measured by Nirvana detector.

4.2. Terahertz Nanoantenna

Methods for fabricating nanometer size structures divide into two categories: top-down and bottom-up approaches. Top-down approach makes small features by cutting down a large building block; focused ion beam (FIB) milling, for example, falls into this group. Here the resolution of the feature depends on effective beam broadening and secondary scattering, leading to reported minimum feature size of five to ten nanometers (34, 35).

Bottom-up approach starts instead with small building blocks and makes desired patterns by stacking the blocks up. In this case a limiting layer, spacer, defines the feature size. Considering that deposition height can be controlled within a few angstroms accuracy (36), bottom-up approach is promising in reducing the feature size of metallic nanostructures down to the extreme. Since the spacer fills the region of highest field enhancement, however, there are some challenges for the bottom-up approach to have applications in sensing or detection.

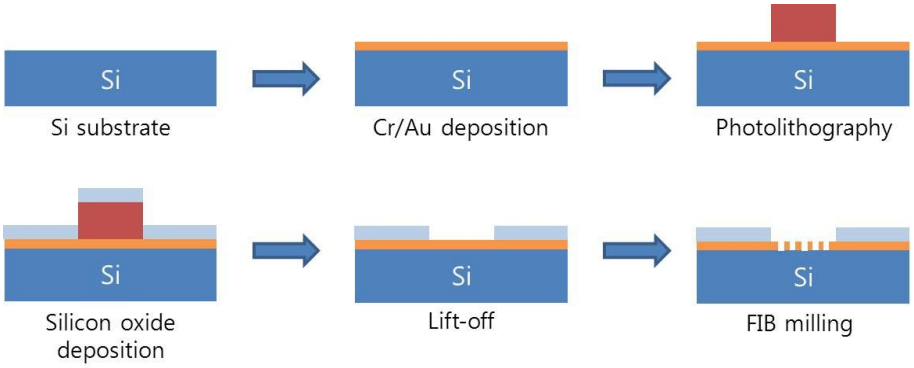

Figure 3 Fabrication of metallic nanoantennas with silicon oxide barrier

In this experiment we use FIB milling process to make metallic nanoantennas, as described in figure 2. On a clean Si substrate, 100nm gold film is deposited with adhesion layer of 5nm chromium. Then photoresist is patterned on the gold film for subsequent silicon oxide deposition of 300nm and lift-off process. This patterned silicon oxide layer works as a barrier for blocking liquid from leaking, which is possible because of the good adhesion between silicon oxide and PDMS. Focused beam of accelerated Ga^{+} ions hits the gold film to form rectangular slots of various sizes.

Figure 3(a) shows the structure of the sample. Antenna length l is 150um, and antenna spacing d_1 and d_2 are 150um and 10um, respectively. Widths of the slots are (b) 400nm, (c) 800nm, (d) 1.3um, and (e) 5um (scale bars: (b) 1um, (c) 2um, (d) 5um, (e) 20um).

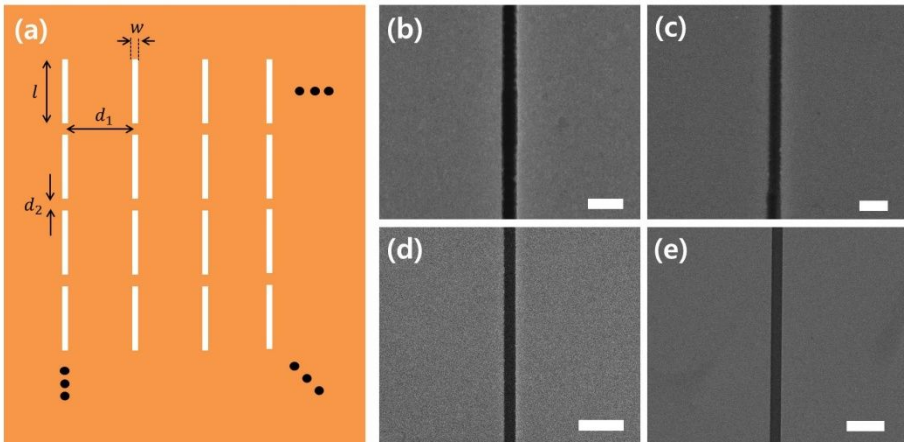

Figure 4 Schematics of the terahertz nanoantenna and the images of the slots

4.3. Cover Layer

In experiments under aqueous conditions, poly-dimethylsiloxane (PDMS) is widely used for its optical transparency, inertness, and convenience in handling (37). This material is especially useful for samples with metallic structures, because when it comes to making a cover layer for the fluidic chamber CMOS techniques such as chemical vapor deposition (CVD) or wafer bonding usually require high temperature or high voltage, which can damage metal layers. One can easily overcome this problem by covering the sample with PDMS, which only needs mild O2 plasma for bonding with silicon dioxide.

For THz spectroscopy, however, PDMS is not such a perfect material for cover layer because it has strong absorption in terahertz regime. Conventional fabrication method of PDMS requires pouring on the master mold, which makes the thickness of PDMS usually ill-defined. This is not a problem in visible frequency, where PDMS is transparent; in terahertz frequency this makes quantitative analysis impossible. Therefore its thickness should be both very small and well-controlled in order for transmission experiment to become

possible. This can be achieved with spin-coating method conventionally used for membrane formation. In this experiment 20um PDMS membrane on 650um thick sapphire substrate is formed with 30 second spin-coating at 3000rpm. Sapphire is also a part of the cover because it prevents the PDMS membrane from inflating. The liquid is then sandwiched between the nanoantenna and the cover layer.

5. Results

5.1. Terahertz Properties of Bulk Liquid

Let $A_0(\omega)$, $A_s(\omega)$ be complex spectra of terahertz wave before and after passing the sample, respectively. Then one can define transfer function of the sample $\mathrm{H_s}(\omega) = A_s(\omega)/A_0(\omega)$ and this value can be calculated from electromagnetic wave's point of view to be as follows (38).

$$H_s(\omega) = exp\left\{i\frac{2\pi d}{\lambda}[n_s(\omega)-1]\right\}exp[-\alpha_s(\omega)d/2]$$

d, $n_s(\omega)$ and $\alpha_s(\omega)$are thickness, refractive index and absorption coefficient of the sample, respectively, and λ is the wavelength of the incident beam. With the phase and amplitude of the complex spectra one can calculate the refractive index and the absorption coefficient of the sample.

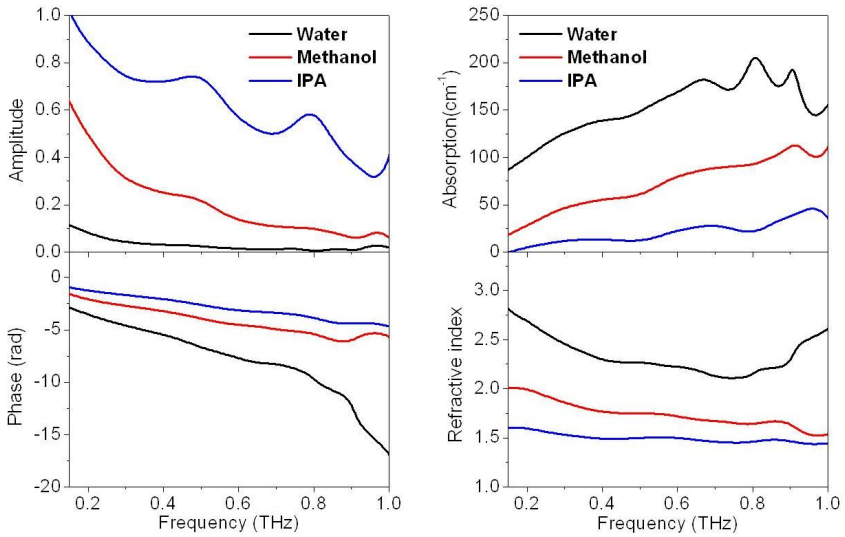

Figure 5 Transmission characteristics and optical properties of water, methanol and IPA

In this experiment three different kinds of liquid – water, methanol, and isopropyl alcohol (IPA) – are used. To measure optical properties of the liquids, a cell with 500um thickness is filled with liquid and its transmission spectrum is measured in time domain. The spectrum is then Fourier-transformed and normalized with respect to spectrum of the cell alone. Figure 3 shows the normalized amplitude and phase of the spectrum (left), and calculated optical properties of the liquids (right). Refractive indices and absorption coefficients are consistent with previously reported values (39), except for those of water above 0.8THz. The deviation is due to small transmission signal at the frequency range.

5.2. Terahertz Nanoantenna Measurement

Calculating the field enhancement inside the nanoantenna follows the method by J. S. Kyoung et al. (40). Using Kirchhoff integral formalism, one can obtain near field enhancement factor from the measured far field according to the following formula.

$$\frac{|<E_n^S(\omega)>|}{|<E_{inc}(\omega)>|} = \frac{\gamma(\omega)\alpha(\omega)}{\beta}$$

Here $\gamma(\omega) = |<E_n^A(\omega)>|/|E_{inc}(\omega)|$ is the field enhancement by the reference aperture, $\alpha(\omega) = |E_f^S(\omega)/E_f^A(\omega)|$ is the ratio between electric field through the sample and electric field through the aperture only, and β is the coverage ratio, i.e. area of the aperture divided by total gap area. The aperture size used for nanoantenna characterization is 1mm X 1mm.

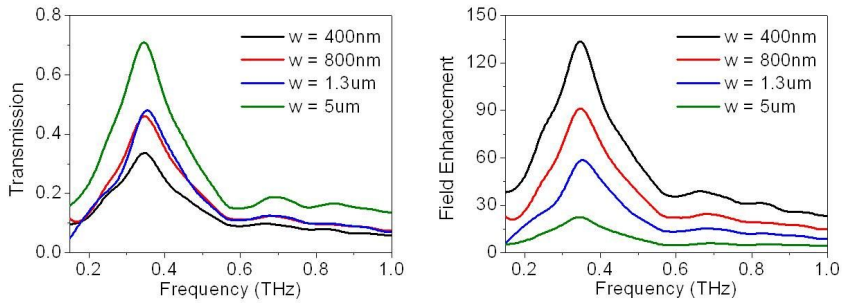

Figure 6 Transmission spectrum and field enhancement factor of terahertz nanoantennas

Figure 4 shows transmission spectra and calculated near field enhancement factor of the terahertz nanoantennas. As the width decreases the transmission also decreases, but in a much less

degree than predicted by general theories (41), clearly showing the existence of field enhancement inside the gap. Since nanoantenna with 400nm width shows the highest near field enhancement factor of 130, this antenna is expected to be the most sensitive to dielectric environment near its structure.

5.3. Water Thin layer on Terahertz Nanoantennas

To check the influence of terahertz nanoantenna on the absorption of the liquids, transmission of thin liquid layer is measured first. The thin liquid layer is formed by sandwiching the liquid between cover layer and silicon substrate patterned with 300nm thick silicon oxide.

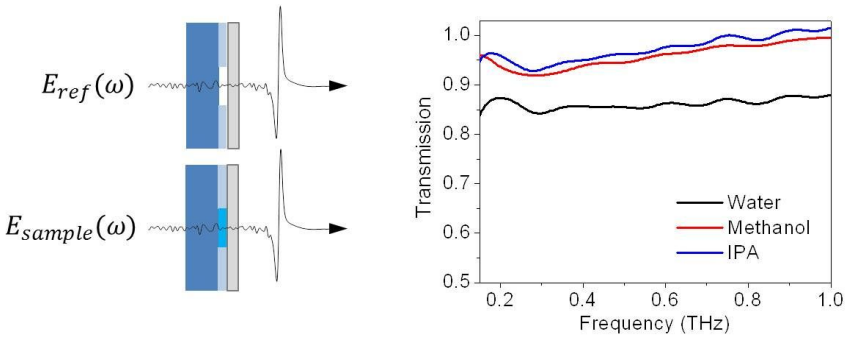

Figure 7 Schematics and results of liquid thin layer transmission experiment

Figure 6 shows the schematics of the experiment and the resulting transmission characteristics. Transmission spectrum of liquid layer is obtained by normalizing the spectrum of the sample $E_{sample}(\omega)$ by spectrum of the substrate with cover layer $E_{ref}(\omega)$. From the absorption spectrum, thickness of the liquids is calculated to be about 25um, 29um, and 103um for water, methanol, and IPA, respectively.

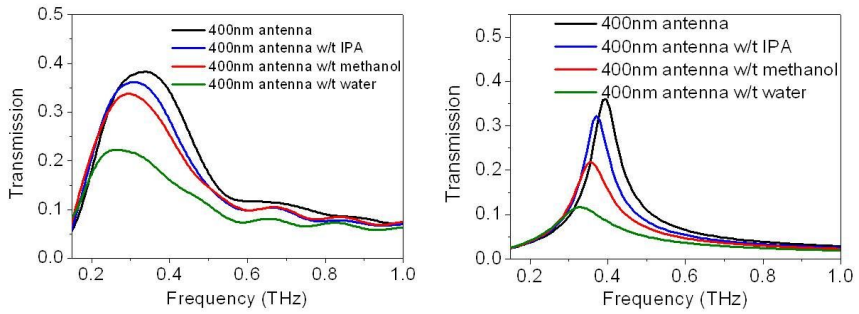

Figure 8 Experimental and theoretical results for liquids on 400nm width terahertz nanoantennas

When a thin liquid layer is put on terahertz nanoantennas, the change in transmission spectrum becomes more distinguishable. Figure 7 shows the experimentally (left) and theoretically (right) obtained transmission spectrums of thin liquids on 400nm width antenna. Before coupling liquid to the nanoantennas 10nm thick silicon oxide layer is coated on the antenna in order to ensure stable formation of liquid layers. Theoretical calculations are performed with experimentally obtained optical parameters at 0.35THz. For the same thickness of target liquids the amplitude modulation has increased from 7% to 12% in case of methanol, and from 15% to 42% for water. Moreover, it is possible to distinguish different liquids by recognizing the red shift of the resonance peak. Experimental results show 8%, 12% and 21% peak shift for IPA, methanol and water, respectively, somewhat larger than predicted values

of 6.5%, 10%, and 17%. The deviations might be due to imperfect sealing or silicon oxide layer, which is the subject for further improvements and study.

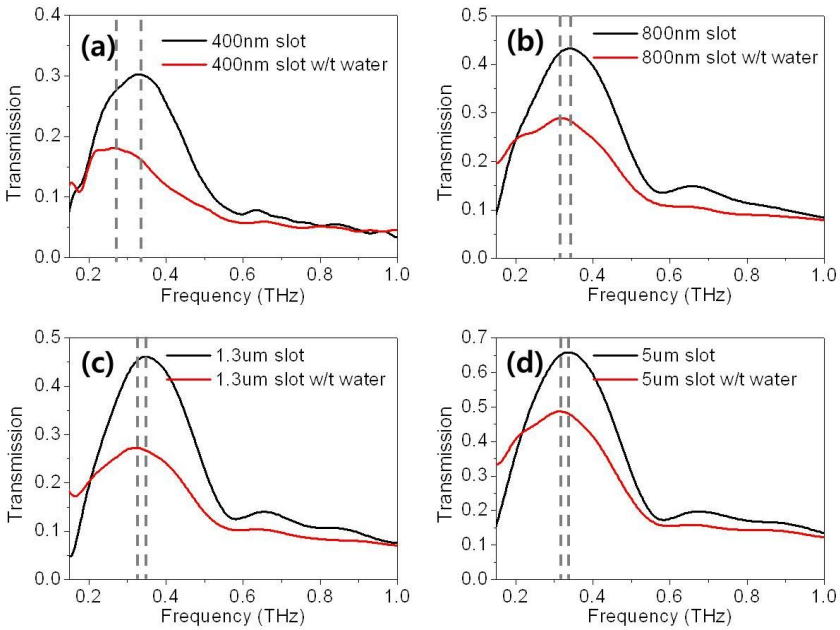

Figure 9 Slot width dependence of transmission of thin water layer on terahertz nanoantennas

Figure 8 shows how the transmission characteristics change as the width of the slot antenna changes. It can be noticed that the amount of peak shift and amplitude modulation both tend to increase as the width of the antennas decreases.

By separating the contribution from liquid inside and outside the slot, one can quantify the absorption enhancement by the slot itself. Assuming that the thickness of the liquid above the antennas is the same as the previously obtained values and

enhanced field is strongly localized inside the slot, one can write

$$T_{total} = T_{slot} \times T_{film}$$

Here T_{total} is the final transmission and T_{film} is assumed to be the same as in figure 6. Expressing T_{slot} in terms of effective absorption coefficient α_{eff} and thickness of the metal d leads to

$$T_{slot} = e^{-\alpha_{eff} d/2}$$

Above formula gives effective absorption coefficient of $7.6 \times 10^4 \mathrm{cm}^{-1}$, $1.1 \times 10^4 cm^{-1}$, and $9.7 \times 10^2 cm^{-1}$ for water, methanol, and IPA. This corresponds to absorption coefficient increase by factor of 590, 220, and 100, respectively. These values are in the same order as the field enhancement inside the slot 130, as expected for electric dipole-dominant absorption processes (17), while additional factors varying from 0.77 to 4.5 need to be investigated further with better controlled experiments.

6. Summary

Metallic nanoantennas are widely used in sensing applications, such as in SEIRA and SERS, for its ability to create hot spots and improve detectability. However, metallic structures have limitations in incorporating fluidic chambers due to its incompatibility with many CMOS techniques. PDMS, the most widely used material in fluidic applications, also suffers from high terahertz absorption. These limitations in combining terahertz nanoantennas with fluidics have forced many experimental schemes to choose reflection geometry.

Avoiding such shortcomings with spin-coated PDMS and silicon oxide barrier, terahertz transmission characteristics of liquids in the presence of metallic nanoantennas can be obtained. When liquid thin layer is coupled with terahertz nanoantennas amplitude modulation and peak shift can be observed, the amount of which depends greatly on the dielectric properties of the liquids. Smaller antenna width also cause in larger peak shift, improving the detectability of the liquids. With improved sealing of the liquid inside the slot and with smaller antenna width, further terahertz transmission experiments on much smaller samples, such as a few-layer water, are expected be possible.

7. References

1. Ritchie RH. Plasma Losses by Fast Electrons in Thin Films. Phys Rev. 1957;106(5):874-81.

2. Ebbesen TW, Lezec HJ, Ghaemi HF, Thio T, Wolff PA. Extraordinary optical transmission through sub-wavelength hole arrays. Nature. 1998;391(6668):667-9.

3. Tanemura T, Balram KC, Ly-Gagnon DS, Wahl P, White JS, Brongersma ML, et al. Multiple-Wavelength Focusing of Surface Plasmons with a Nonperiodic Nanoslit Coupler. Nano letters. 2011;11(7):2693-8.

4. Smith DR, Pendry JB, Wiltshire MCK. Metamaterials and negative refractive index. Science. 2004;305(5685):788-92.

5. Pendry JB, Martin-Moreno L, Garcia-Vidal FJ. Mimicking surface plasmons with structured surfaces. Science. 2004;305(5685):847-8.

6. Garcia-Vidal FJ, Martin-Moreno L, Ebbesen TW, Kuipers L. Light passing through subwavelength apertures. Rev Mod Phys. 2010;82(1):729-87.

7. Fleischm.M, Hendra PJ, Mcquilla.Aj. Raman-Spectra of Pyridine Adsorbed at a Silver Electrode. Chemical Physics Letters. 1974;26(2):163-6.

8. Smith ED, G. Modern Raman Spectroscopy: A Practical Approach: John Wiley and Sons; 2005.

9. Miki A, Ye S, Osawa M. Surface-enhanced IR absorption on platinum nanoparticles: an application to real-time monitoring of electrocatalytic reactions. Chem Commun. 2002(14):1500-1.

10. Fischer BM, Walther M, Jepsen PU. Far-infrared vibrational modes of DNA components studied by terahertz time-domain spectroscopy. Phys Med Biol. 2002;47(21):3807-14.

11. Fitch MJ, Leahy-Hoppa MR, Ott EW, Osiander R. Molecular absorption cross-section and absolute absorptivity in the THz frequency range for the explosives TNT, RDX, HMX, and PETN. Chemical Physics Letters. 2007;443(4-6):284-8.

12. Le F, Brandl DW, Urzhumov YA, Wang H, Kundu J, Halas NJ, et al. Metallic nanoparticle arrays: A common substrate for both surface-enhanced Raman scattering and surface-enhanced infrared absorption. Acs Nano. 2008;2(4):707-18.

13. Wu CH, Khanikaev AB, Adato R, Arju N, Yanik AA, Altug H, et al. Fano-resonant asymmetric metamaterials for ultrasensitive spectroscopy and identification of molecular monolayers. Nature materials. 2012;11(1):69-75.

14. Kang JH, Choe JH, Kim DS, Park QH. Substrate effect

on aperture resonances in a thin metal film. Opt Express. 2009;17(18):15652-8.

15. Rosman C, Prasad J, Neiser A, Henkel A, Edgar J, Sonnichsen C. Multiplexed Plasmon Sensor for Rapid Label-Free Analyte Detection. Nano letters. 2013;13(7):3243-7.

16. Kravets VG, Schedin F, Jalil R, Britnell L, Gorbachev RV, Ansell D, et al. Singular phase nano-optics in plasmonic metamaterials for label-free single-molecule detection. Nature materials. 2013;12(4):304-9.

17. Park HR, Ahn KJ, Han S, Bahk YM, Park N, Kim DS. Colossal Absorption of Molecules Inside Single Terahertz Nanoantennas. Nano letters. 2013;13(4):1782-6.

18. Jackson JD. Classical Electrodynamics. 3rd ed: John Wiley & Sons inc; 1999.

19. Park QH. Optical antennas and plasmonics. Contemp Phys. 2009;50(2):407-23.

20. Garcia-Vidal FJ, Moreno E, Porto JA, Martin-Moreno L. Transmission of light through a single rectangular hole. Physical Review Letters. 2005;95(10).

21. Seo MA, Adam AJL, Kang JH, Lee JW, Jeoung SC, Park QH, et al. Fourier-transform terahertz near-field imaging of one-dimensional slit arrays: mapping of electric-field-,

magnetic-field-, and Poynting vectors. Opt Express. 2007;15(19):11781-9.

22. Park HR, Koo SM, Suwal OK, Park YM, Kyoung JS, Seo MA, et al. Resonance behavior of single ultrathin slot antennas on finite dielectric substrates in terahertz regime. Applied Physics Letters. 2010;96(21).

23. Seo MA, Park HR, Koo SM, Park DJ, Kang JH, Suwal OK, et al. Terahertz field enhancement by a metallic nano slit operating beyond the skin-depth limit. Nature Photonics. 2009;3(3):152-6.

24. Chen X, Park HR, Pelton M, Piao X, Lindquist NC, Im H, et al. Atomic layer lithography of wafer-scale nanogap arrays for extreme confinement of electromagnetic waves. Nature communications. 2013;4:2361.

25. Kang JH, Kim DS, Park QH. Local Capacitor Model for Plasmonic Electric Field Enhancement. Physical Review Letters. 2009;102(9).

26. Moskovits M. Surface-Enhanced Raman Spectroscopy: a Brief Perspective. Surface-Enhanced Raman Scattering - Physics and Applications2006. p. 1-18.

27. Han PY, Zhang XC. Coherent, broadband midinfrared terahertz beam sensors. Applied Physics Letters.

1998;73(21):3049-51.

28. Zhang W, Azad AK, Grischkowsky D. Terahertz studies of carrier dynamics and dielectric response of n-type, freestanding epitaxial GaN. Applied Physics Letters. 2003;82(17):2841-3.

29. Huber R, Tauser F, Brodschelm A, Bichler M, Abstreiter G, Leitenstorfer A. How many-particle interactions develop after ultrafast excitation of an electron-hole plasma. Nature. 2001;414(6861):286-9.

30. Besnard M, Delcampo N, Yarwood J, Catlow B. Far-Infrared Spectroscopy of Liquid Benzene - Long-Ranged and Short Ranged Dynamics in the Neat Liquid and in Solution. J Mol Liq. 1994;62:33-54.

31. Pedersen JE, Keiding SR. Thz Time-Domain Spectroscopy of Nonpolar Liquids. Ieee J Quantum Elect. 1992;28(10):2518-22.

32. Heyden M, Sun J, Funkner S, Mathias G, Forbert H, Havenith M, et al. Dissecting the THz spectrum of liquid water from first principles via correlations in time and space. Proceedings of the National Academy of Sciences of the United States of America. 2010;107(27):12068-73.

33. Planken PCM, Nienhuys HK, Bakker HJ, Wenckebach T.

Measurement and calculation of the orientation dependence of terahertz pulse detection in ZnTe. J Opt Soc Am B. 2001;18(3):313-7.

34. Broers AN, Hoole ACF, Ryan JM. Electron beam lithography - Resolution limits. Microelectron Eng. 1996;32(1-4):131-42.

35. Orloff J, Swanson LW, Utlaut M. Fundamental limits to imaging resolution for focused ion beams. J Vac Sci Technol B. 1996;14(6):3759-63.

36. Puurunen RL. Surface chemistry of atomic layer deposition: A case study for the trimethylaluminum/water process. Journal of Applied Physics. 2005;97(12).

37. McDonald JC, Duffy DC, Anderson JR, Chiu DT, Wu HK, Schueller OJA, et al. Fabrication of microfluidic systems in poly(dimethylsiloxane). Electrophoresis. 2000;21(1):27-40.

38. Zhang JQ, Grischkowsky D. Terahertz time-domain spectroscopy of submonolayer water adsorption in hydrophilic silica aerogel. Opt Lett. 2004;29(9):1031-3.

39. Kindt JT, Schmuttenmaer CA. Far-infrared dielectric properties of polar liquids probed by femtosecond terahertz pulse spectroscopy. Journal of Physical Chemistry. 1996;100(24):10373-9.

40. Kyoung JS, Seo MA, Park HR, Ahn KJ, Kim DS. Far field detection of terahertz near field enhancement of sub-wavelength slits using Kirchhoff integral formalism. Optics Communications. 2010;283(24):4907-10.

41. Bethe HA. Theory of diffraction by small holes. Phys Rev. 1944;66(7/8):163-82.

국 문 초 록

금속 나노슬랏 안테나 위에 형성된 얇은 액체막의 테라헤르츠파 투과 특성을 탐구하였다. 나노슬랏 안테나는 금속막에 나노미터 너비의 구멍이 나 있는 구조를 말하는데, 특정 주파수에서 공명 현상을 보이고 투과 특성이 주변 매질에 민감하게 반응하는 특성을 가지고 있다. 얇은 액체막은 스핀코팅된 PDMS와 이산화실리콘 구조물을 활용하여 액체가 새어나오는 것을 방지함으로써 형성하였다. 나노슬랏 안테나 위에 액체막을 형성한 후 테라헤르츠파를 투과시켰을 때 그 액체의 광학적 특성에 따라 안테나의 투과도가 줄고 공명 주파수가 이동하는 현상을 관측하였다. 이 현상은 나노슬랏 안테나의 너비가 좁아질수록 강해지는 경향을 보였다. 액체를 가두는 기술을 더 발전시키고 안테나의 구조를 잘 조절한다면 이 실험으로 수 개의 분자막과 같이 아주 작은 시료도 분석할 수 있으리라 전망한다.

주요어 : 테라헤르츠 분광학, 액체, 나노슬랏 안테나
학 번 : 2012-20387